European Journal of Neuroscience (2003) 18(4):879-886.

Nigral GABAergic inhibition upon cholinergic neurons in the rat pedunculopontine tegmental nucleus

Saitoh, Kazuya ; Hattori, Satoko ; Song, Wen-Jie ; Isa, Tadashi ; Takakusaki, Kaoru.

Receiving Editor: T. TAKAHASHI

Title

Nigral GABAergic inhibition upon cholinergic neurons in the rat pedunculopontine tegmental nucleus

Authors

Kazuya Saitoh[1], Satoko Hattori[2], Wen-Jie Song[2], Tadashi Isa[3], and Kaoru Takakusaki[1]

Affiliation

1 *Department of Physiology, Asahikawa Medical College, Asahikawa 078-8510,* **2** *Department of Electronic Engineering, Graduate School of Engineering, Osaka University, Suita 565-0821,* **3** *Department of Integrative Physiology, National Institute for Physiological Sciences, Okazaki 444-8585, Japan*

Running title

NIGRAL INHIBITION UPON PPN CHOLINERGIC NEURONS (49 chara.& spaces)

Number of pages: **33 pages**

Number of Figures: **6 figures**

Number of Tables: **0**

Number of equations: **0**

Number of words in:

the whole manuscript: **6342 words**

the Abstract: **204 words**

the introduction: **349 words**

Correspondence: **K.Takakusaki**

Department of Physiology, Asahikawa Medical College,

2-1-1 Midorigaoka-Higashi, Asahikawa 078-8510, Japan

Telephone number: +81-166-68-2332

Facsimile number: +81-166-68-2339

E-mail: kusaki@asahikawa-med.ac.jp

Key Words: substantia nigra pars reticulata; GABA receptor; basal ganglia; whole-cell patch-clamp recording; single-cell reverse transcription-PCR

Abstract

We investigated, in a midbrain parasagittal slice preparation of Wistar rats (postnatal day 9 to 17), the synaptic inhibition of neurons in the pedunculopontine tegmental nucleus (PPN) which was mediated by gamma (γ)-amino-butyric acid (GABA). Whole-cell patch-clamp recording was used, in combination with a single-cell reverse transcription-polymerase chain reaction amplification technique, to record synaptic potentials and to identify the phenotype of the recorded PPN neuron. In the presence of the ionotropic glutamate receptor antagonists, 6-cyano-2, 3-dihydroxy-7-nitro-quinoxaline-2, 3, dione, and $_{DL}$-2-amino-5-phosphonovaleric acid, single electrical stimuli were applied to the substantia nigra pars reticulata (SNr), one of the basal ganglia output nuclei. Stimulation of the SNr evoked inhibitory postsynaptic potentials (IPSPs) in 73 of the 104 neurons in the PPN. The IPSPs were abolished with a $GABA_A$ receptor antagonist, bicuculline. Inhibitory postsynaptic currents of the neurons were reversed in polarity at approximately –93.5 mV, which was close to the value of the equilibrium potential for chloride ions of -88.4 mV. Single-cell reverse transcription-polymerase chain reactions revealed that approximately 30% (9/32) of the PPN neurons that received inhibition from the SNr expressed detectable levels of choline acetyltransferase mRNA. These findings show that output from the SNr regulates the activity of cholinergic PPN neurons through $GABA_A$ receptors.

Introduction

The pedunculopontine tegmental nucleus (PPN), which consists of both cholinergic and non-cholinergic neurons, is located in the dorsolateral mesopontine tegmentum. The PPN has been implicated in a variety of functions including locomotion (Mogenson *et al*., 1989; Garcia-Rill, 1991), muscular tonus (Lai & Siegel, 1990; Takakusaki *et al*., 2003), visually guided saccades (Aizawa *et al*., 1999; Kobayashi *et al*., 2002), and the regulation of the sleep-wake cycles (Jones, 1991; Steriade, 1992).

Neuroanatomically, the PPN receives dense efferents from the substantia nigra pars reticulata (SNr), one of the basal ganglia output nuclei in rats (Beckstead *et al*., 1979; Rye *et al*., 1987; Spann & Grofova, 1992). Although light microscopic studies have demonstrated that nigral efferents to the PPN terminate more preferentially on non-cholinergic neurons than cholinergic neurons (Rye *et al*., 1987; Steininger *et al*., 1997), an electron microscopic study has shown that the nigral terminals are distributed also to cholinergic PPN neurons (Grofova & Zhou, 1998). These findings support the notion that the SNr-PPN projection plays an important role in controlling the functions noted above (for review, see Inglis & Winn, 1995). To understand the functional significance of the basal ganglia-PPN system therefore, requires an examination on how the nigral efferents act on the PPN cholinergic neurons.

Electrophysiological studies have demonstrated that stimuli applied to the SNr can induce monosynaptic inhibitory effects on PPN neurons in both *in vivo* (Noda & Oka,

1984; Granata & Kitai, 1991) and *in vitro* (Kang & Kitai, 1990; Takakusaki *et al*., 1997b) preparations. However, these studies have not yet elucidated which type of GABA receptors are involved in the SNr-induced inhibition of the PPN neurons. Whether the inhibition is exerted not only on non-cholinergic neurons, but also on cholinergic neurons, is also unresolved.

The present study was designed to answer the issues outlined above. The SNr-induced inhibition of the PPN neurons was investigated by using whole-cell patch-clamp recording in the rat midbrain slices. After identification of GABAergic inhibition from the SNr, a technique involving a single-cell reverse transcription-polymerase chain reaction (RT-PCR) was used to determine whether, or not, the recorded PPN neurons were cholinergic.

Materials and methods

The experiments were approved by the Committee for Animal Experimentation at Asahikawa Medical College, at Osaka University and at Okazaki National Institute.

Slice preparations

A total of 51 Wistar rats (postnatal day 9 to 17) were deeply anesthetized with diethylether and then decapitated. The brain was quickly removed and submerged in an ice-cold cutting solution which was bubbled with a gas mixture of 95% O_2 and 5% CO_2 from 5 to 8 minutes. Midbrain slices (400 to 500 μm thick) were then prepared as described previously (Isa *et al*., 1998) along the parasagittal plane so as to contain both the SNr and PPN. Horizontal slices (300 μm thick) containing the subthalamic nucleus were also used in control experiments (see below). A microslicer (Microslicer, DTK 2000, Dosaka EM, Kyoto, Japan) was used to cut the slices which were then incubated in artificial cerebrospinal fluid (ACSF). The solution was bubbled with a gas mixture of 95% O_2 and 5% CO_2 at room temperature for more than 1 hour before recording. After incubation, a slice was mounted in a recording chamber and continuously superfused with the ACSF (2 to 3 ml/min) at room temperature. In some experiments, NaCl was replaced with Na-gluconate so that the concentration of chloride ion in the ACSF ($[Cl^-]_{out}$) was reduced (low-chloride ACSF).

Whole-cell patch-clamp recording

Records were obtained from 104 PPN neurons using the whole-cell patch-clamp

technique (Edwards *et al.*, 1989). The patch pipettes were guided with micromanipulators under visual control to contact neurons in the slice using video images obtained with an IR-CCD camera (C2400-79H, Hamamatsu photonics, Hamamatsu, Japan) attached to an upright microscope (Axioskop FS, Zeiss, Gottingen, Germany, or ECLIPSE E-600-FN, Nikon, Tokyo, Japan). An EPC-7 (HEKA, Lambrecht, Germany) or Axoclamp 200B (Axon Instruments, Foster City, CA) patch-clamp amplifier was used. The location of the neurons was estimated from the video images. On the basis of the video images we constructed a map of the neurons in the PPN area from which data were obtained (Fig.5E). The pipettes were filled with a solution (described below) which had an osmolarity of 280 to 290 mOsm/l. The resistance of the electrodes was from 2.5 to 4.0 MΩ in the bath solution. The series resistance during recording was from 6 to 15 MΩ and was routinely compensated by 70 to 80%. Data were acquired using a pClamp system (Axon Instruments). Because the liquid junction potential between the ACSF and the pipette internal solution was estimated to be -15 mV, the actual membrane potential was corrected by this value. When using low-chloride ACSF, the membrane potential was corrected by a liquid junction potential of –12 mV. Five cathodal, concentric bipolar electrodes (Clark Electromedical Instruments, Pangbourne, UK) were placed in a linear array so that both the inside and outside of the SNr could be stimulated (Fig. 4A). The electrical stimulation consisted of a single pulse, and from 2 to 50 pulses, with a duration of 0.2 ms, and a frequency of 10

to 100 Hz. We determined the appropriate stimulus strength for every neuron (Fig.3A). If stimuli with an intensity of 1 mA failed to induce any inhibitory effects, we ceased any further investigation on that neuron.

Single-cell RT-PCR procedure

To test if the recorded PPN neurons were cholinergic, single-cell RT-PCR analysis was performed to detect choline acetyltransferase (ChAT) mRNA. The patch electrode was filled with approximately 5 μl of sterile intracellular solution. After recording, the cytoplasm was aspirated with a negative pressure and under visual guidance, into the patch electrode. Sterile gloves were worn during the procedure to minimize RNase contamination. The RT procedure and the primers for ChAT have been described previously (Song *et al*., 1998). The predicted size of the amplified ChAT cDNA is 324 base pairs. A thermal cycler (MJ Research, Inc., Watertown, MA) was used for PCR. The reaction mixture contained 2.5 mM $MgCl_2$, 0.5 mM of each of the deoxynucleotide triphosphates, 1 μM primers, 2.5 U Taq DNA polymerase (Promega, Madison, WI), 5 μl 10X Buffer (Promega) and the cellular cDNA from the RT reaction. After denaturing at 94°C (10 minutes), the reaction was cycled 45 times at 94°C for 1 minute, 58°C for 1 minute, and 72°C for 1 minute. This procedure was followed by a ten minute extension at 72°C. The PCR products were separated by electrophoresis in 2% agarose gel and visualized by staining with ethidium bromide. In representative cases, amplicons were purified from the gel (QIAquick Gel Extraction Kit, QIAGEN, Germany), sequenced

with a dye termination procedure and examined to see if they matched the published sequence (Brice *et al*., 1989). Negative controls for contamination from extraneous DNA were run for every batch of neurons by replacing the cellular template with water. These controls were consistently negative. Negative controls for genomic DNA were not performed because the cell nucleus was not aspirated and that genomic DNA has been shown not to affect the results of single-cell RT-PCR experiments (Johansen *et al*., 1995). To verify that our protocol actually identifies cholinergic neurons, we used subthalamic neurons for negative controls. Subthalamic neurons are glutamatergic (Kitai & Kita, 1987), and thus are not expected to express ChAT mRNA. Subthalamic neurons could be visually identified under the microscope (Otsuka et al., 2001), because the region does not contain interneurons.

Solution and drugs

The cutting solution contained (in mM): 234 sucrose; 2.5 KCl; 1.25 NaH_2PO_4; 10 $MgSO_4$; 0.5 $CaCl_2$; 26 $NaHCO_3$; and 11 glucose. The ACSF contained (in mM): 125 NaCl; 2.5 KCl; 2 $CaCl_2$; 1 $MgCl_2$; 26 $NaHCO_3$; 1.25 NaH_2PO_4; and 25 glucose. The low-chloride ACSF contained (in mM): 62.5 NaCl; 62.5 Na-gluconate; 2.5 KCl; 2 $CaCl_2$; 1 $MgCl_2$; 26 $NaHCO_3$; 1.25 NaH_2PO_4; and 25 glucose. The internal solution of the pipettes contained (in mM): 160 K-gluconate; 0.2 EGTA; 2 $MgCl_2$; 2 Na_2-ATP; 10 HEPES; 0.1 spermine; and 0.5 Na-GTP (the pH was adjusted to 7.3). The DL-2-amino-5-phosphonovaleric acid (AP-5) and bicuculline methiodide were purchased

from Sigma-Aldrich Japan (Tokyo, Japan). The 6-cyano-7-nitroquinoxaline-2, 3-dione disodium (CNQX) and P-3-aminopropyl-P-diethoxymethyl phosphinic acid (CGP 35348) was supplied by TOCRIS/Nacalai (Kyoto, Japan).

Results

Electrophysiological identification of the PPN neurons

Whole cell recordings were made from a total of 104 PPN neurons. The mean resting membrane potential was –72.0 ± 7.3 mV (mean ± S.D.).

Three types of mesopontine cholinergic neurons have been classified in rats. The three classifications which have been reported by Kamondi et al. (1992), and which are based on the intrinsic membrane properties of the neurons include: (i) neurons with a low threshold Ca^{2+} spike (LTS); (ii) neurons with a transient outward current (A-current); and (iii) neurons with both an LTS and an A-current. These criteria were applied to the PPN neurons recorded in this study. A representative example of these neurons is shown in Fig. 1. In a current clamp condition, this neuron displayed a burst of action potentials riding on an LTS (indicated by an open arrowhead) after the offset of hyperpolarizing current pulses (Fig. 1A). In the voltage clamp recordings, transient inward currents were induced by applying a test pulse-potential of –60 mV after a prepulse-potential of 400 ms that was varied from –90 to –60 mV (Fig. 1Ba). These inward currents could possibly be attributed to the activation of the low threshold Ca^{2+} channels. When the voltage command, which was comprised of a hyperpolarizing prepulse to –130 mV for 400 ms and test pulses with potentials of –80 mV to –50 mV, was applied, an A-current was elicited (Fig. 1Bb). However, voltage trajectories due to the A-current, including a delay in the return of the membrane potential to the baseline

following hyperpolarizing current pulses (Leonard & Llinás, 1994), were not necessarily prominent in the current clamp recording. Both current and voltage clamp recordings were therefore obtained in most neurons to test whether each neuron had an A-current and/or an LTS.

Effective sites for evoking inhibitory effects on the PPN neurons

In the presence of AP-5 (50 μM) and CNQX (10 μM), stimuli applied to the SNr evoked inhibitory postsynaptic currents (IPSCs) on the PPN neurons. A representative example was shown in Fig. 2A. This neuron displayed both an A-current and an LTS in the voltage clamp condition (Fig. 2Aa). A latency of around 5 ms and a 10-90% rise time of approximately 1.5 ms were displayed by an SNr-induced IPSC (Fig. 2Ab).

Then we estimated the optimal nigral stimulus sites for evoking inhibitory postsynaptic effects on PPN neurons. We stimulated inside and outside the SNr using a linear array of five stimulating electrodes. The distance between the tip of each adjacent electrode was 300 μm. The array of electrodes was arranged as shown in Fig. 2B. The electrodes were placed on the ventral part of the SNr (#1), the middle part of the SNr (#2), the dorsal part of the SNr (#3), and the mesencephalic reticular formation (#4 and #5). Representative examples are shown in Fig. 2C. In one neuron, IPSCs were induced when electrical stimuli were applied to the SNr (Fig. 2Ca, filled arrowheads). In another neuron, a prominent IPSC was induced by stimuli applied to the outside of the SNr (Fig. 2Cb, an open arrowhead). On the basis of the optimal sites for stimuli to evoke

inhibitory effects, the PPN neurons were divided into two groups (Fig. 2B). In one group of neurons, the inhibitory effects were preferentially induced by intranigral (#1-3) stimulation (Group I: n = 73). On the other hand, in the other group of neurons (Group II: n = 31) inhibitory effects were rather produced by extranigral stimulation (#4-5). In the right column of Fig. 2B, the normalized amplitude of the IPSCs were plotted against the number of stimulating electrodes in ten neurons of each group. In the present study, analyses were performed on only Group I neurons. The following examinations were then made on the inhibitory effects that were induced by stimuli through an electrode placed in the middle part of the SNr (#2).

Characteristics of SNr-induced inhibitory effects on the PPN neurons

In the PPN neuron illustrated in Fig.3Aa, SNr stimulation induced IPSCs with a latency of around 5 ms. The amplitude of the IPSCs increased as the stimulus strength was increased (Fig. 3Aa). However, the amplitude of the IPSCs was saturated if a stimulus strength of more than 500 μA was delivered to the SNr (Fig. 3Ab). Therefore the stimulus strength was set below 500 μA for this neuron. In this neuron, frequency of the SNr stimuli were also altered (Fig. 3B). The latency of the IPSCs remained constant in response to each stimulus pulse when either the strength or the frequency of the SNr stimuli was changed. Therefore, the inhibitory effects were considered to be monosynaptically evoked from the SNr.

The reversal potentials of the IPSCs were examined in 37 neurons (Fig. 4). In

all of the neurons, the amplitude of the IPSCs was reduced as the membrane potential was hyperpolarized. However, a prominent outward rectification was usually observed. Because this rectification made an accurate measurement of the reversal potential difficult, we obtained a clear reversal from only eight neurons. An example is shown in Fig. 4Aa. The IPSC polarity was reversed between –90 and –100 mV. The I-V relationship for each neuron is superimposed in Fig. 4Ab. The reversal potential of the IPSCs (E_{IPSC}) was close to the equilibrium potential of chloride ions (-88.4 mV, indicated by an open arrowhead), and had a value of –93.5 ± 8.4 mV (mean ± S.D.; Fig. 4Ab). To determine the Cl^- ion selectivity of the IPSCs more rigorously, we estimated the E_{IPSC} under low $[Cl^-]_{out}$ in three neurons. With 133.5 mM $[Cl^-]_{out}$ (ACSF), the IPSCs were reversed at approximately –90 mV (Fig. 3Ba). As $[Cl^-]_{out}$ was reduced to 71.0 mM (low-chloride ACSF), the E_{IPSC} shifted to approximately –74 mV (Fig. 4Ba). The E_{IPSC} estimated under each external solution was plotted against semilogarithmic co-ordinates (Fig. 4Bb). These values of the E_{IPSC} agreed approximately with the equilibrium potentials of chloride ions which were calculated from the Nernst equation (straight line in Fig. 4Bb).

GABAergic nature of the SNr-induced IPSPs

As a next step of this study, we examined whether the inhibitory effects were mediated by GABA receptors. Representative findings are shown in Fig. 5A-C where SNr stimulation induced inhibitory postsynaptic potentials (IPSPs) in three types of neurons;

(i) neurons with an LTS, (ii) neurons with an A-current, and (iii) neurons with both an LTS and an A-current. Because the IPSPs in each type of neuron were completely abolished by an application of bicuculline (30 μM; Fig. 5A-C, row b), the inhibitory effects were considered to be mediated via $GABA_A$ receptors.

It has been demonstrated that stronger stimuli were required to elicit $GABA_B$ receptor-mediated IPSPs in neurons in the thalamus (von Krosigk *et al*., 1999) and in the hippocampus (Otis *et al*., 1993). We therefore applied prolonged and high frequency stimuli to the SNr and investigated whether $GABA_B$ receptors were involved in the generation of the IPSPs (Fig. 5D). A bath application of a selective $GABA_B$ receptor antagonist, CGP 35348 (100 μM) did not change the time course and the amplitude of IPSPs. It was observed that the IPSPs were completely abolished by a further application of bicuculline (30 μM). Essentially the same findings were observed in all 73 neurons, which indicated that the $GABA_B$ receptors did not significantly contribute to the SNr-induced IPSPs.

In Fig. 5E, the locations of the PPN neurons, which received the nigral inhibitory effect, are plotted on a representative parasagittal plane of the brainstem. The SNr stimulation induced IPSPs in 15 neurons with an LTS (denoted by filled triangles), 36 neurons with an A-current (open circles), and 22 neurons with both an A-current and an LTS (hatched squares). These neurons were rostrocaudally distributed throughout the whole of the PPN.

Cholinergic nature of the PPN neurons

After identification of the GABAergic inhibitory effects, the cholinergic nature was examined in 32 PPN neurons (Fig. 6). In the PPN neuron in Fig. 6A, stimulation of the SNr elicited an IPSP (Fig. 6B). The expression of ChAT mRNA was detected by single-cell RT-PCR amplification in this neuron (Fig. 6C). In nine of the 32 (28.1%) PPN neurons, ChAT mRNA was detected. Of these nine neurons, one had only LTS, seven had an A-current, and one had both an LTS and an A-current (Fig. 6D). As a negative control, the expression of ChAT mRNA was studied in 13 subthalamic neurons; none of the neurons was ChAT-positive.

Discussion

The present study clearly demonstrated that SNr stimulation produced $GABA_A$-receptor mediated inhibitory effects on cholinergic PPN neurons. Before consideration of the role of this inhibitory connection, the present experimental procedures are discussed.

Consideration of the experimental procedures

We have shown that SNr stimulation inhibited approximately 70% (73/104) of the PPN neurons. This finding is consistent with neuroanatomical studies which have indicated that the PPN receives a dense GABAergic input from the SNr (Beckstead *et al*., 1979; Edley & Graybiel, 1983; Rye *et al*., 1987; Spann & Grofova, 1992). However it was important to confirm that the GABAergic inhibition in the PPN neurons was arising from the SNr. To overcome this problem, we placed stimulating electrodes on both the intranigral and extranigral areas so that the optimal sites for evoking inhibitory effects on the PPN neurons could be determined. In some neurons, inhibition was more effectively induced from extranigral areas than from intranigral areas (Fig.2, Group II). It has been shown that the pallidotegmental and striatotegmental fibers preferentially pass through the extranigral area (Nauta *et al*., 1978; Jackson & Crossman, 1983; Shink *et al*., 1997). Effects of intranigral stimuli on Group II neurons could thus be ascribed to the activation of not only cell bodies but also fibers of passage described above. Our analysis therefore was restricted to Group I neurons.

In the neuron shown in Fig. 2Ca, stimuli through the electrodes placed on the

mesencephalic reticular formation (#4-5) did not induce IPSCs at a strength of 1 mA (data not shown). Thus the extent of current spread due to a maximal stimulus strength (1 mA) was less than 300 μm, which was the distance between the tip of adjacent electrodes. Moreover we determined an appropriate stimulus strength for every neuron (Fig. 3A). Thus we deduced that the current spread due to the stimulus strength in this study was confined mostly to the vicinity of the stimulus electrode tip. Consequently, we consider that the GABAergic inhibition observed in this study would actually originate from the SNr.

The reversal potential of the SNr-induced IPSCs was –93.5 mV, which is close to the value of the equilibrium potential for Cl^- ions of -88.4 mV. However, reversal potentials in two neurons were under –100 mV. This value is close to the equilibrium potential for K^+ ions of -104.5 mV. Even so, IPSCs in these neurons would be mediated by Cl^- ions, because the IPSCs were diminished by an application of the $GABA_A$ receptor antagonist, bicuculline. The value of the E_{IPSC} depolarized under the low-chloride ACSF (Fig.4B) further supports the evidence that the IPSCs are selectively mediated by Cl^- ions. Therefore we consider that the lack of a space clamp could be involved with the variation of the reversal potentials. Grofova & Zhou (1998) demonstrated nigral synapses terminated on both proximal and distal dendritic areas. Then the area of postsynaptic membrane at the GABAergic synapses would not be isopotential with the soma from which whole-cell recordings were obtained.

The present results revealed that cholinergic PPN neurons do receive a nigral GABAergic input. However, the ChAT mRNA could be detected in only about 30% (9/32) of the neurons with GABAergic inputs. This may reflect the neuroanatomical findings that GABAergic afferents from the basal ganglia to the PPN are preferentially on non-cholinergic neurons rather than cholinergic neurons (Rye *et al*., 1987; Spann & Grofova, 1992). Nevertheless, it should be noted that some experimental conditions might affect this incidence of the cholinergic nature of the PPN neurons. First, technical limitations such as an incomplete harvesting of the cytoplasm may result in an underestimate of the percentage of cholinergic neurons. Second, the age of the animals used in the present study (postnatal day 9 to 17) may also have affected the results because it has been suggested that the NADPH diaphorase-positive (cholinergic) PPN neurons in rats has been suggested to mature after an age of two weeks (Skinner *et al*., 1989).

The present study revealed ChAT mRNA in all three types of PPN neurons. This observation may support the previous findings by Kamondi *et al*. (1992) about the neurons of the laterodorsal tegmental nucleus (LDT) of young rats (postnatal day 9 to 15). They demonstrated that 40% of neurons with only LTS, in addition to 64% of neurons with an A-current, were identified as cholinergic by using NADPH-diaphorase histochemistry. However, the present finding is inconsistent with the reports that in adult animals cholinergic neurons have been found only in neurons with an A-current of

the rat PPN (Kang & Kitai, 1990; Takakusaki & Kitai, 1997a) and the guinea pig LDT (Leonard & Llinás, 1994). This inconsistency could be explained by the postnatal development of the A-current of cholinergic neurons. Song *et al*. (2000) have demonstrated that the A-current in rat striatal cholinergic neurons is up-regulated during postnatal development. A similar phenomenon may occur in the PPN cholinergic neurons. In young rats the ChAT positive neurons which have only an LTS might express an A-current during the process of postnatal development, and might then at maturity be classified as neurons with both an A-current and an LTS.

Functional implication of the nigral GABAergic inhibition on the PPN neurons

Kang & Kitai (1990) have reported that when *in vitro* preparations were used a burst firing was not observed in the cholinergic neurons but was found in non-cholinergic neurons. In contrast, the cholinergic neurons have a regular firing property which is maintained by a combination of Ca^{2+} ion- dependent and Na^{+} ion-dependent pacemaker conductances (Takakusaki & Kitai, 1997a). Garcia-Rill & Skinner (1988) also observed that in a fictive locomotor preparation in cats, a bursting activity of the PPN neurons was linked to the locomotor cycles whereas a tonic firing activity was preferentially related to the initiation and/or termination of the locomotion. On the other hand, Steriade *et al*. (1990) demonstrated that burst-firing neurons in both the PPN and the LDT increased their discharge rates during wakefulness and REM sleep but not during a non-REM sleep period. The slow and regular firing cells, in contrast, increased their

firing rates from wakefulness to non-REM sleep and increased their discharge even more during REM sleep. Based on these findings the cholinergic and non-cholinergic neurons may have different functions. Accordingly, the GABAergic basal ganglia output from the SNr to the PPN could be involved in the expression of a variety of functions such as locomotion and behavioral states (sleep-wake cycles) by modulating the activity of both the cholinergic and the non-cholinergic PPN neurons.

Acknowledgments

This work was performed under a Joint Research Program between National Institute for Physiological Sciences, Osaka University, and Asahikawa Medical College.

This work was supported by a Grant-in-Aid for Scientific Research (C) to K.S., Grant-in-Aid for Scientific Research (C) to W.J.S., grants from the Ministry of Education, Sports, Culture, Science and Technology and CREST (Core Research for the Evolution Science and Technology) of the Japan Science and Technology Corporation, Mitsubishi Foundation to T.I., and Grants-in-Aid for Scientific Research (C), Priority Areas (A) and a grant from Japan Science and Technology Corporation to K.T.

Abbreviations

$[Cl^-]_{in}$, concentration of chloride ion in the internal solution of the pipettes

$[Cl^-]_{out}$, concentration of chloride ion in the artificial cerebrospinal fluid

ACSF, artificial cerebrospinal fluid

AP-5, $_{DL}$-2-amino-5-phosphonovaleric acid

CGP 35348, P-3-aminopropyl-P- diethoxymethyl phosphinic acid

ChAT, choline acetyltransferase

CNQX, 6-cyano-7-nitroquinoxaline-2, 3-dione disodium

E_{IPSC}, reversal potential of inhibitory postsynaptic current

GABA, gamma (γ)-amino-butyric acid

IPSC, inhibitory postsynaptic current

IPSP, inhibitory postsynaptic potential

LDT, laterodorsal tegmental nucleus

LTS, low threshold Ca^{2+} spike

PPN, pedunculopontine tegmental nucleus

RT-PCR, reverse transcription-polymerase chain reaction

SNr, substantia nigra pars reticulata

Figure legends

Fig. 1. Electrophysiological identification of a neuron in the pedunculopontine tegmental nucleus (PPN). A. In the current clamp condition, a low-threshold Ca^{2+} spike (LTS; an open arrowhead) was displayed after the offset of a 200-pA hyperpolarizing current command. B. (a) In the voltage clamp recordings, transient inward currents were displayed by applying a test pulse-potential of –60 mV after a prepulse-potential with a duration of 400 ms that was varied between –90 to –60 mV in increments of 5 mV. (b) Transient outward currents (A-currents) were also observed following a hyperpolarizing prepulse of up to –130 mV for 400 ms which was then stepped to a series of potentials from –80 to –50 mV in increments of 5 mV. Each trace illustrated in Ba and Bb is an average of 3 sweeps.

Fig. 2. Effective sites for evoking inhibitory effects on PPN neurons. A. (a) An example of a neuron with an A-current and an LTS. In the voltage clamp recordings, both transient outward currents (a filled arrowhead) and transient inward current (an open arrowhead) were displayed by applying a test pulse-potential of –65 mV following a prepulse-potential with a duration of 400 ms that was varied between –95 to –65 mV in increments of 5 mV. (b) Stimulation of the SNr (an arrow) induced inhibitory postsynaptic current (IPSC) in the presence of antagonists for ionotropic glutamate receptors (50 μM APV and 10 μM CNQX). In this neuron, the latency (*) was around 5

ms, and the10-90% rise time (**) was around 1.5 ms. B. A linear array of five stimulating electrodes was placed both inside and outside the SNr, and the effects of stimulation through these electrodes were investigated. (*right*) Locations of stimulating electrodes (shaded circles). (*left*) Stimulus effects were divided into two classes. In Group I neurons (filled circles), inhibitory effects were preferentially induced by intranigral stimulation. However stimuli applied to the outside of the SNr effectively induced inhibitory actions in Group II neurons (open circles). In each group, the mean value (circles) and standard error (bars) of the normalized amplitude of the IPSCs were obtained from 10 PPN neurons. C. Representative examples of Group I (a) and Group II (b) neurons. Each trace is an average of 5 sweeps. Filled (a) and open (b) arrowheads indicate IPSCs evoked by intranigral and extranigral stimuli, respectively. The current and time calibrations in Ca also apply to Cb. Cb, cerebellum; ML, medial lemniscus; PPN, pedunculopontine tegmental nucleus; SNr, substantia nigra pars reticulata; Sp, superior cerebellar peduncle.

Fig. 3. Inhibitory effects on PPN neurons induced by stimulating the substantia nigra pars reticulata (SNr). A. Stimulation of the SNr (an arrow) induced IPSCs in the presence of antagonists for ionotropic glutamate receptors (50 μM AP-5 and 10 μM CNQX). (a) The amplitude of the IPSCs increased as the stimulus strength was increased. Each trace is an average of 5 sweeps. (b) The amplitude of the IPSCs

saturated at a stimulation strength of more than 500 μA in this neuron. B. Repetitive pulse stimulation evoked IPSCs with a fixed latency of approximately 5 ms (black bar). Each trace is an average of 5 sweeps.

Fig. 4. Chloride ion selectivity of SNr-induced IPSCs. A. (a) The traces are superimpositions of IPSCs at different holding potential (V_h) levels between -50 and -110 mV. Each trace is an average of 4 sweeps. (b) Superimposition of I-V curves of eight neurons. The reversal potential was –93.5 ± 8.4 mV, and is close to the equilibrium potential of Cl^- ion (E_{Cl}, an open arrowhead). B. (a) I-V curves of the IPSCs with 4.0 mM $[Cl^-]_{in}$ in 133.5 mM $[Cl^-]_{out}$ (dotted line with filled circles) and in 71.0 mM $[Cl^-]_{out}$ (solid line with open circles). Each circle and bar shows a mean value and the standard error, respectively. These were obtained from 9 trials of 3 neurons. (b) The reversal potential of IPSCs plotted against the logarithmic ratio of external and internal Cl^- ion concentrations ($[Cl^-]_{out}/[Cl^-]_{in}$). A straight line was drawn according to the Nernst equation for the equilibrium potential of Cl^- ions.

Fig. 5. The SNr-induced GABAergic inhibitory postsynaptic potentials (IPSPs) in three types of PPN neurons. A-C. The upper traces (a) are electrophysiological identifications of each type of PPN neuron. Open arrowheads indicate LTS. Filled arrowheads indicate the voltage trajectories that were due to A-current. The lower traces

(b) are superimpositions of SNr-induced effects on each PPN neuron before (Control) and after application of bicuculline (Bic; 30 μM). The voltage and time calibrations in Aa also apply to Ba and Ca, and the calibrations in Ab also apply to Bb and Cb. D. Superimpositions of the membrane responses of a PPN neuron induced by repetitive SNr stimuli (dotted line; 10 pulses, 100 Hz, 400 μA) in the control condition, in the presence of CGP 35348 (100 μM), and in the presence of both CGP 35348 (100 μM) and bicuculline (30 μM). Each trace is an average of 3 sweeps. E. The location of recorded neurons in the PPN. The filled triangles, open circles, and hatched squares indicate neurons with only LTS, neurons with an A-current, and neurons with both an A-current and an LTS, respectively.

Fig. 6 Cholinergic nature of the PPN neurons indicated by a single-cell RT-PCR procedure. A. An example of a neuron having an A-current. Filled and open arrowheads indicate the voltage trajectories that underlie the A-current after the onset of depolarizing current pulse, and after the offset of a hyperpolarizing current pulse, respectively. B. An SNr-induced IPSP in the presence of AP-5 (50 μM) and CNQX (10 μM). C. Choline acetyltransferase (ChAT) mRNA was detected with a single-cell RT-PCR procedure. D. The frequency of the ChAT mRNA positive PPN neurons (filled bar) and negative PPN neurons (open bar) in relation to the electrophysiological phenotypes.

References

Aizawa, H., Kobayashi, Y., Yamamoto, M. & Isa, T. (1999) Injection of nicotine into the superior colliculus facilitates occurrence of express saccades in monkeys. *J Neurophysiol*, **82**, 1642-1646.

Beckstead, R.M., Domesick, V.B. & Nauta, W.J. (1979) Efferent connections of the substantia nigra and ventral tegmental area in the rat. *Brain Res*, **175**, 191-217.

Brice, A., Berrard, S., Raynaud, B., Ansieau, S., Coppola, T., Weber, M.J. & Mallet, J. (1989) Complete sequence of a cDNA encoding an active rat choline acetyltransferase: a tool to investigate the plasticity of cholinergic phenotype expression. *J Neurosci Res*, **23**, 266-273.

Edley, S.M. & Graybiel, A.M. (1983) The afferent and efferent connections of the feline nucleus tegmenti pedunculopontinus, pars compacta. *J Comp Neurol*, **217**, 187-215.

Edwards, F.A., Konnerth, A., Sakmann, B. & Takahashi, T. (1989) A thin slice preparation for patch clamp recordings from neurones of the mammalian central nervous system. *Pflugers Arch*, **414**, 600-612.

Garcia-Rill, E. (1991) The pedunculopontine nucleus. *Prog Neurobiol*, **36**, 363-389.

Garcia-Rill, E. & Skinner, R.D. (1988) Modulation of rhythmic function in the posterior midbrain. *Neuroscience*, **27**, 639-654.

Granata, A.R. & Kitai, S.T. (1991) Inhibitory substantia nigra inputs to the

pedunculopontine neurons. *Exp Brain Res*, **86**, 459-466.

Grofova, I. & Zhou, M. (1998) Nigral innervation of cholinergic and glutamatergic cells in the rat mesopontine tegmentum: light and electron microscopic anterograde tracing and immunohistochemical studies. *J Comp Neurol*, **395**, 359-379.

Inglis, W.L. & Winn, P. (1995) The pedunculopontine tegmental nucleus: where the striatum meets the reticular formation. *Prog Neurobiol*, **47**, 1-29.

Isa, T., Endo, T. & Saito, Y. (1998) The visuo-motor pathway in the local circuit of the rat superior colliculus. *J Neurosci*, **18**, 8496-8504.

Jackson, A. & Crossman, A.R. (1983) Nucleus tegmenti pedunculopontinus: efferent connections with special reference to the basal ganglia, studied in the rat by anterograde and retrograde transport of horseradish peroxidase. *Neuroscience*, **10**, 725-765.

Johansen, F.F., Lambolez, B., Audinat, E., Bochet, P. & Rossier, J. (1995) Single cell RT-PCR proceeds without the risk of genomic DNA amplification. *Neurochem Int*, **26**, 239-243.

Jones, B.E. (1991) Paradoxical sleep and its chemical/structural substrates in the brain. *Neuroscience*, **40**, 637-656.

Kamondi, A., Williams, J.A., Hutcheon, B. & Reiner, P.B. (1992) Membrane properties of mesopontine cholinergic neurons studied with the whole-cell patch-clamp technique: implications for behavioral state control. *J Neurophysiol*, **68**,

1359-1372.

Kang, Y. & Kitai, S.T. (1990) Electrophysiological properties of pedunculopontine neurons and their postsynaptic responses following stimulation of substantia nigra reticulata. *Brain Res*, **535**, 79-95.

Kitai, S.T. & Kita, H. (1987) Anatomy and physiology of the subthalamic nucleus: a driving force of the basal ganglia. In Carpenter, M.B. & Jayaraman, A. (eds), *The Basal Ganglia II*. Plenum, New York, pp. 357-373.

Kobayashi, Y., Inoue, Y., Yamamoto, M., Isa, T. & Aizawa, H. (2002) Contribution of pedunculopontine tegmental nucleus neurons to performance of visually guided saccade tasks in monkeys. *J Neurophysiol*, **88**, 715-731.

Lai, Y.Y. & Siegel, J.M. (1990) Muscle tone suppression and stepping produced by stimulation of midbrain and rostral pontine reticular formation. *J Neurosci*, **10**, 2727-2734.

Leonard, C.S. & Llinás, R. (1994) Serotonergic and cholinergic inhibition of mesopontine cholinergic neurons controlling REM sleep: an *in vitro* electrophysiological study. *Neuroscience*, **59**, 309-330.

Mogenson, G.J., Wu, M. & Tsai, C.T. (1989) Subpallidal-pedunculopontine projections but not subpallidal-mediodorsal thalamus projections contribute to spontaneous exploratory locomotor activity. *Brain Res*, **485**, 396-398.

Nauta, W.J., Smith, G.P., Faull, R.L. & Domesick, V.B. (1978) Efferent connections and

nigral afferents of the nucleus accumbens septi in the rat. *Neuroscience*, **3**, 385-401.

Noda, T. & Oka, H. (1984) Nigral inputs to the pedunculopontine region: intracellular analysis. *Brain Res*, **322**, 332-336.

Otis, T.S., De Koninck, Y. & Mody, I. (1993) Characterization of synaptically elicited $GABA_B$ responses using patch-clamp recordings in rat hippocampal slices. *J Physiol*, **463**, 391-407.

Otsuka T., Murakami F. & Song W.J. (2001) Excitatory postsynaptic potentials trigger a plateau potential in rat subthalamic neurons at hyperpolarized states. *J Neurophysiol*, **86**,1816-1825.

Rye, D.B., Saper, C.B., Lee, H.J. & Wainer, B.H. (1987) Pedunculopontine tegmental nucleus of the rat: cytoarchitecture, cytochemistry, and some extrapyramidal connections of the mesopontine tegmentum. *J Comp Neurol*, **259**, 483-528.

Shink, E., Sidibe, M. & Smith, Y. (1997) Efferent connections of the internal globus pallidus in the squirrel monkey: II. Topography and synaptic organization of pallidal efferents to the pedunculopontine nucleus. *J Comp Neurol*, **382**, 348-363.

Skinner, R.D., Conrad, C., Henderson, V., Gilmore, S.A. & Garcia-Rill, E. (1989) Development of NADPH diaphorase-positive pedunculopontine nucleus neurons. *Exp Neurol*, **104**, 15-21.

Song, W.J., Hattori, S. & Murakami, F. (2000) Postnatal development of the A-type potassium current in rat striatal cholinergic interneurons. *Neurosci. Res.*, **Supplement 24**, S 81.

Song, W.J., Tkatch, T., Baranauskas, G., Ichinohe, N., Kitai, S.T. & Surmeier, D.J. (1998) Somatodendritic depolarization-activated potassium currents in rat neostriatal cholinergic interneurons are predominantly of the A type and attributable to coexpression of Kv4.2 and Kv4.1 subunits. *J Neurosci*, **18**, 3124-3137.

Spann, B.M. & Grofova, I. (1992) Cholinergic and non-cholinergic neurons in the rat pedunculopontine tegmental nucleus. *Anat Embryol (Berl)*, **186**, 215-227.

Steininger, T.L., Wainer, B.H. & Rye, D.B. (1997) Ultrastructural study of cholinergic and noncholinergic neurons in the pars compacta of the rat pedunculopontine tegmental nucleus. *J Comp Neurol*, **382**, 285-301.

Steriade, M. (1992) Basic mechanisms of sleep generation. *Neurology*, **42**, 9-17; discussion 18.

Steriade, M., Datta, S., Pare, D., Oakson, G. & Curro Dossi, R.C. (1990) Neuronal activities in brain-stem cholinergic nuclei related to tonic activation processes in thalamocortical systems. *J Neurosci*, **10**, 2541-2559.

Takakusaki, K., Habaguchi, T., Ohinata-Sugimoto, J., Saitoh, K. & Sakamoto, T. (2003) Basal ganglia efferents to the brainstem centers controlling postural muscle tone

and locomotion: A new concept for understanding motor disorders in basal ganglia dysfunction. *Neuroscience*, **119**, 293-308.

Takakusaki, K. & Kitai, S.T. (1997a) Ionic mechanisms involved in the spontaneous firing of tegmental pedunculopontine nucleus neurons of the rat. *Neuroscience*, **78**, 771-794.

Takakusaki, K., Shiroyama, T. & Kitai, S.T. (1997b) Two types of cholinergic neurons in the rat tegmental pedunculopontine nucleus: electrophysiological and morphological characterization. *Neuroscience*, **79**, 1089-1109.

von Krosigk, M., Monckton, J.E., Reiner, P.B. & McCormick, D.A. (1999) Dynamic properties of corticothalamic excitatory postsynaptic potentials and thalamic reticular inhibitory postsynaptic potentials in thalamocortical neurons of the guinea-pig dorsal lateral geniculate nucleus. *Neuroscience*, **91**, 7-20.

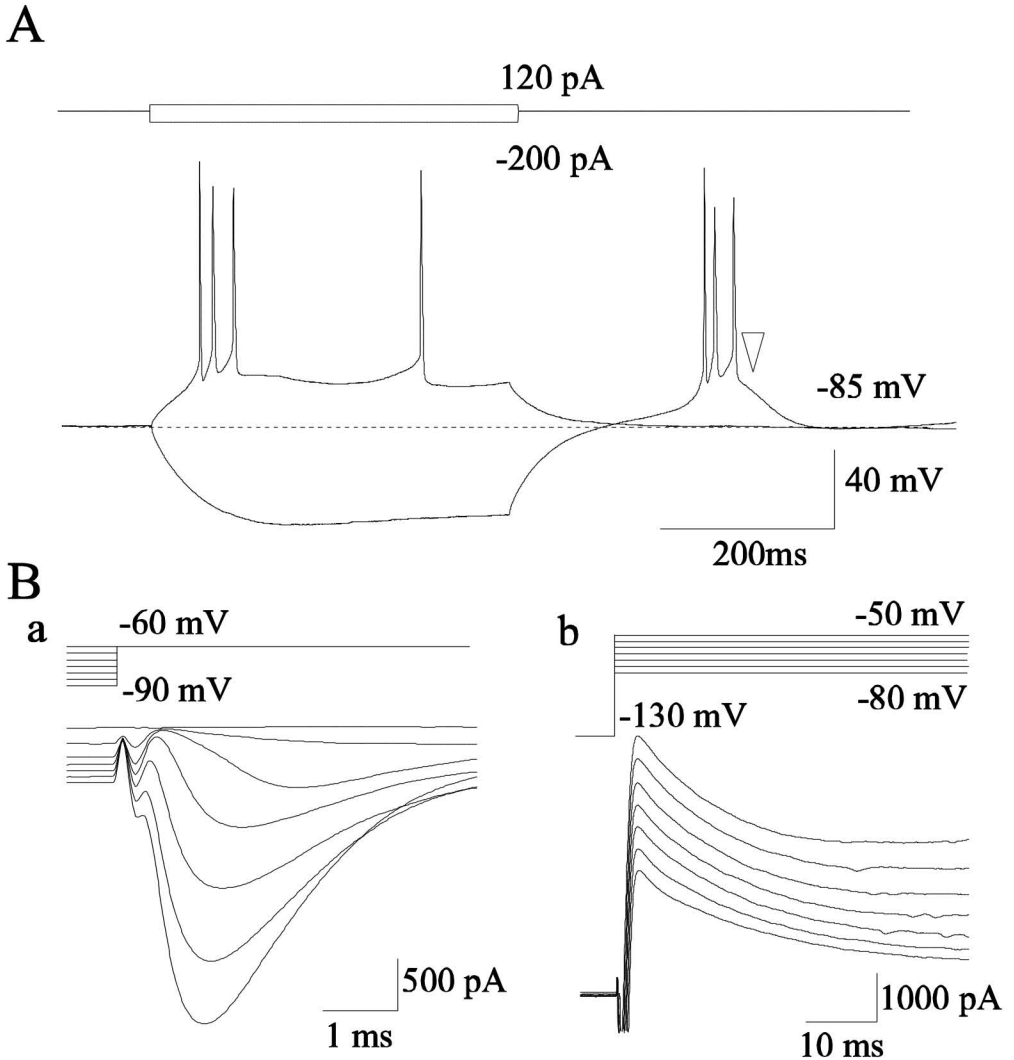
A
120 pA
-200 pA
-85 mV
40 mV
200ms
B
a
-60 mV
-90 mV
500 pA
1 ms
b
-50 mV
-80 mV
-130 mV
1000 pA
10 ms

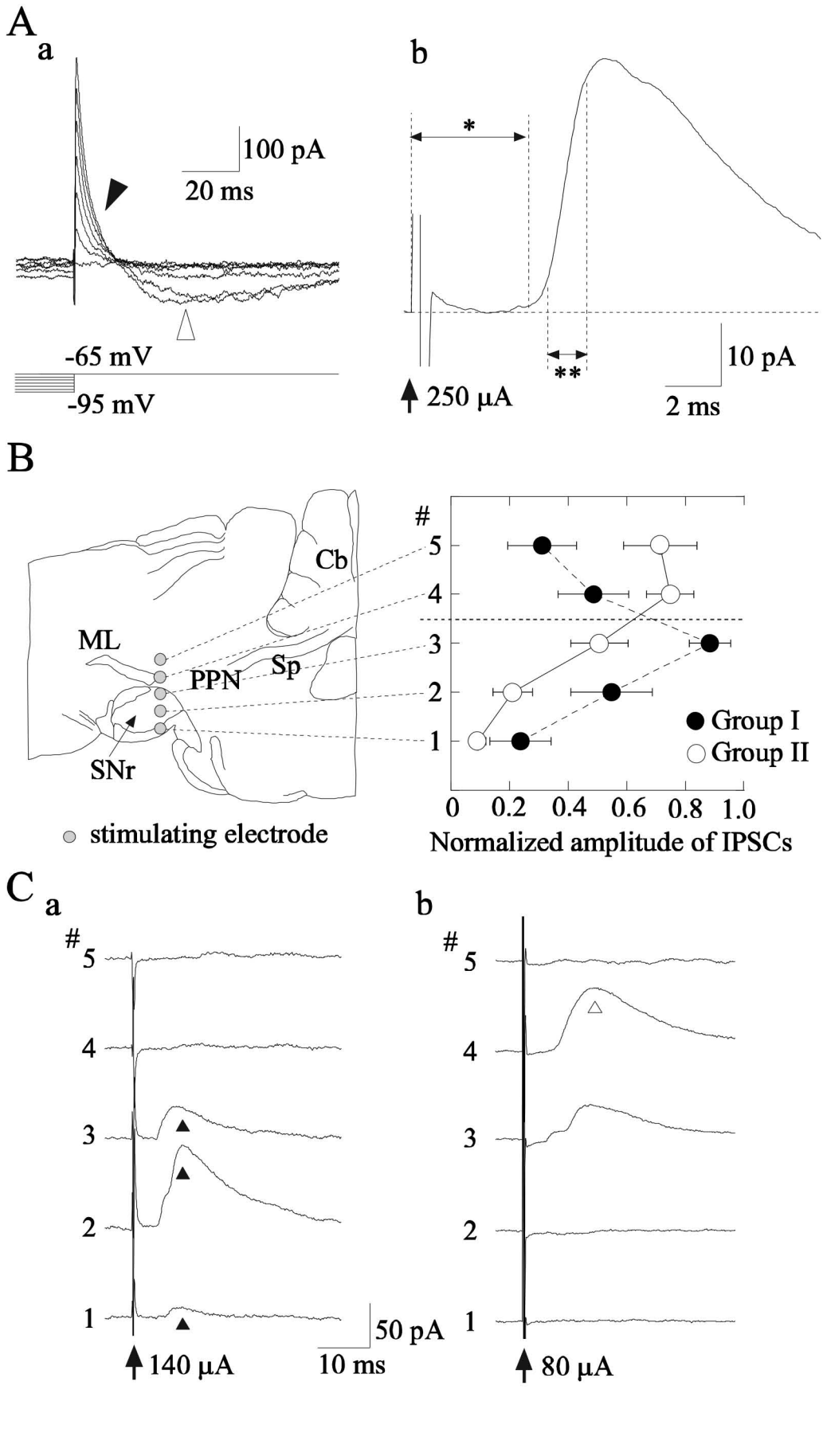
A
a
100 pA
20 ms
-65 mV
-95 mV
b
*
**
10 pA
250 µA
2 ms
B
Cb
ML
PPN
Sp
SNr
stimulating electrode
#
5
4
3
2
1
Group I
Group II
0
0.2
0.4
0.6
0.8
1.0
Normalized amplitude of IPSCs
C
a
b
#
5
4
3
2
1
50 pA
10 ms
140 µA
80 µA

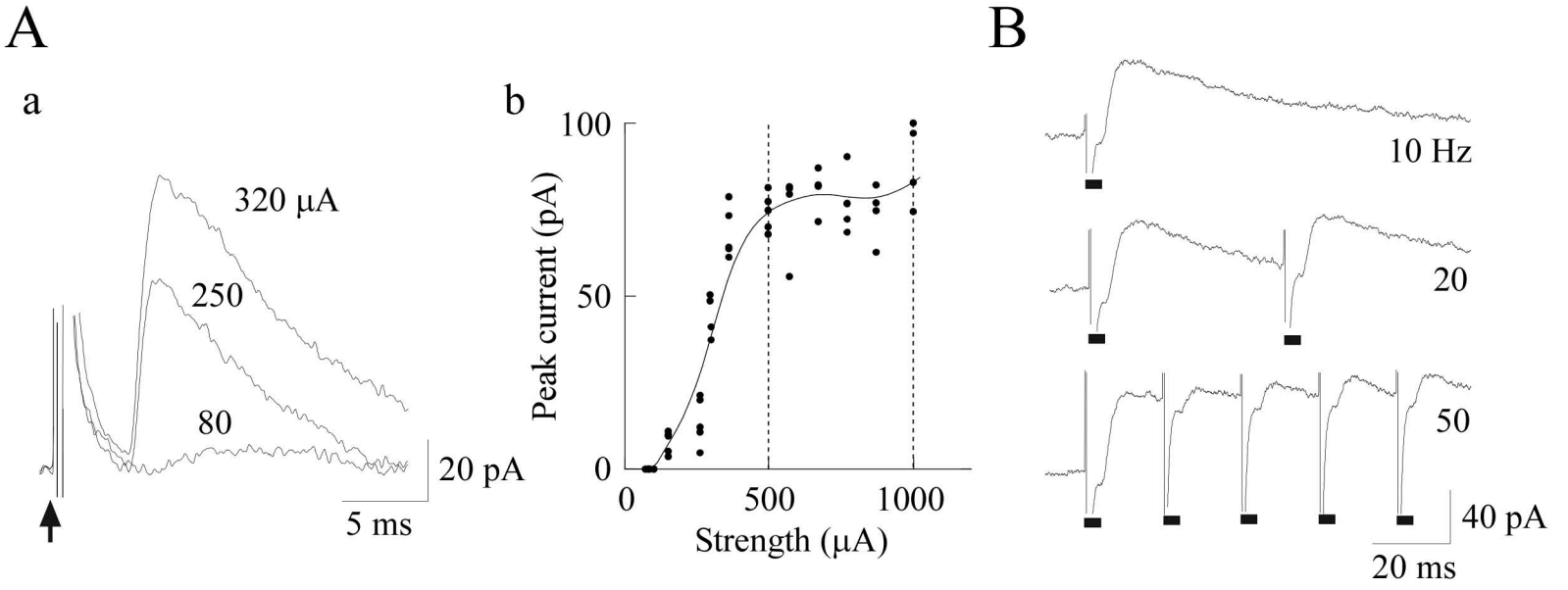
A
a
320 μA
250
80
20 pA
5 ms
b
100
50
0
Peak current (pA)
0
500
1000
Strength (μA)
B
10 Hz
20
50
40 pA
20 ms

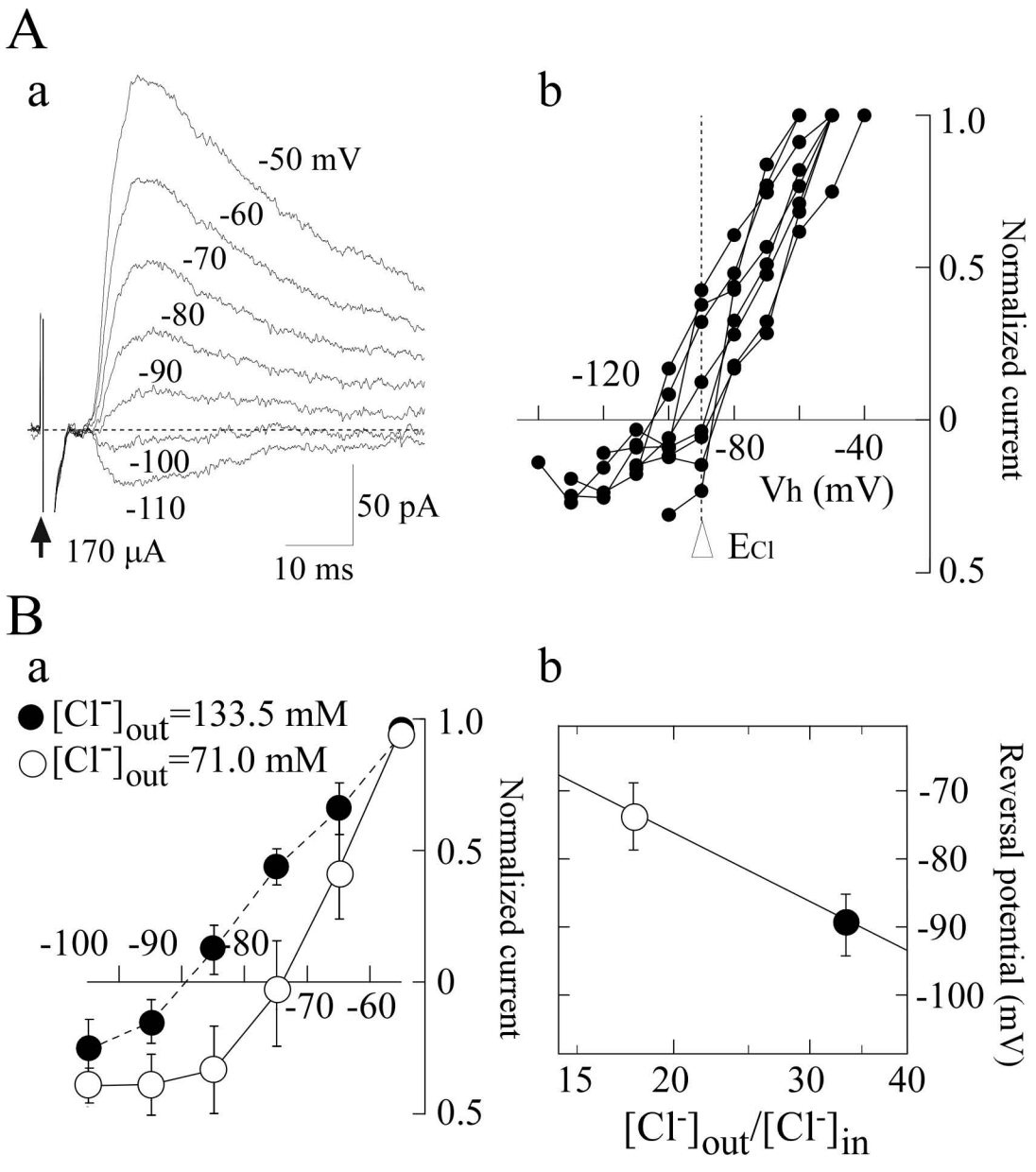
A
a
-50 mV
-60
-70
-80
-90
-100
-110
50 pA
170 μA
10 ms
b
1.0
0.5
0
0.5
-120
-80
-40
Vh (mV)
ECl
Normalized current
B
a
[Cl-]out=133.5 mM
[Cl-]out=71.0 mM
1.0
0.5
0
0.5
-100 -90 -80
-70 -60
Normalized current
b
-70
-80
-90
-100
15
20
30
40
[Cl-]out/[Cl-]in
Reversal potential (mV)

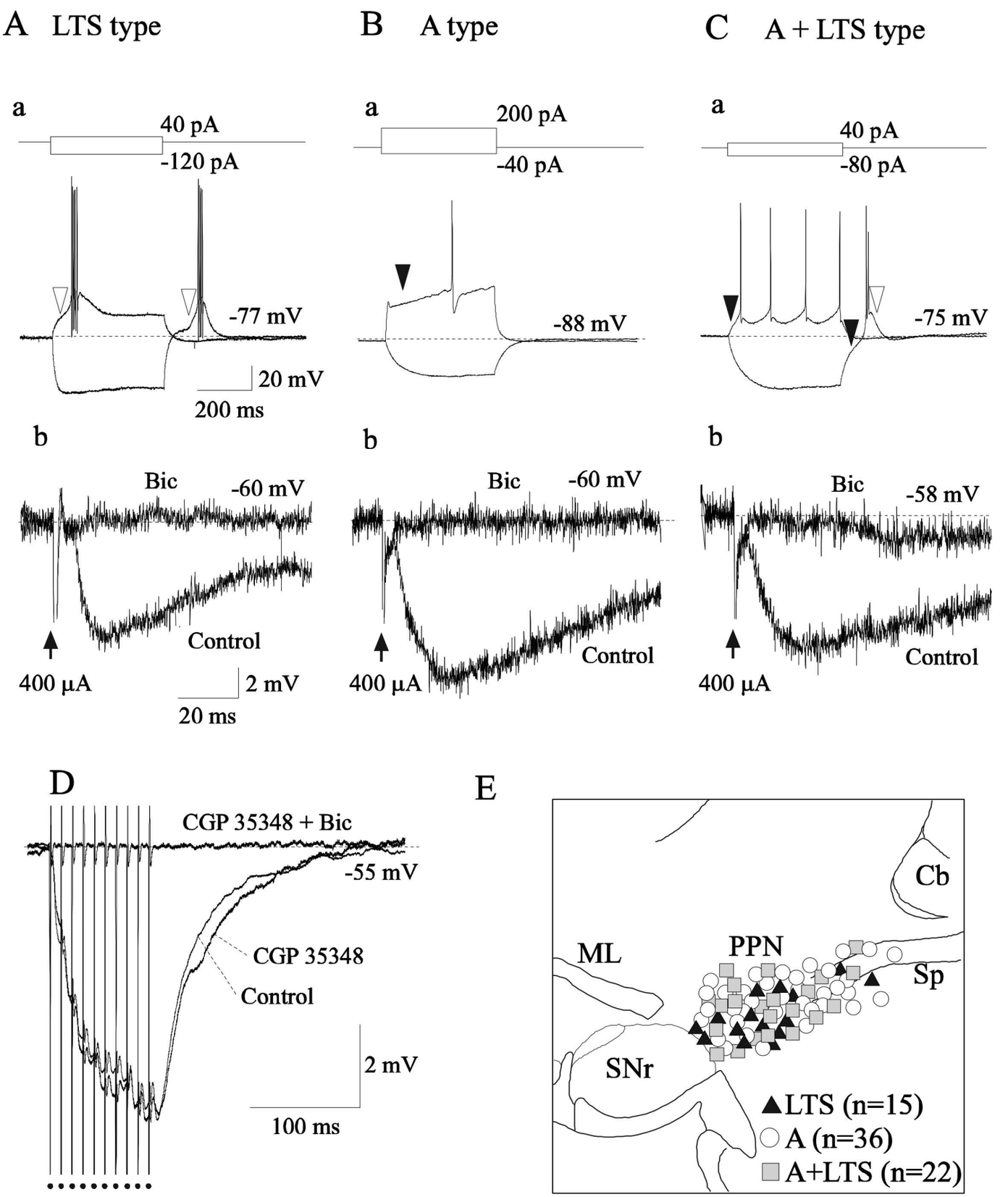
A LTS type
B A type
C A + LTS type
a
40 pA
-120 pA
-77 mV
20 mV
200 ms
200 pA
-40 pA
-88 mV
-80 pA
-75 mV
b
Bic
-60 mV
Control
400 µA
2 mV
20 ms
-58 mV
D
CGP 35348 + Bic
-55 mV
CGP 35348
Control
2 mV
100 ms
E
Cb
ML
PPN
Sp
SNr
▲LTS (n=15)
A (n=36)
A+LTS (n=22)

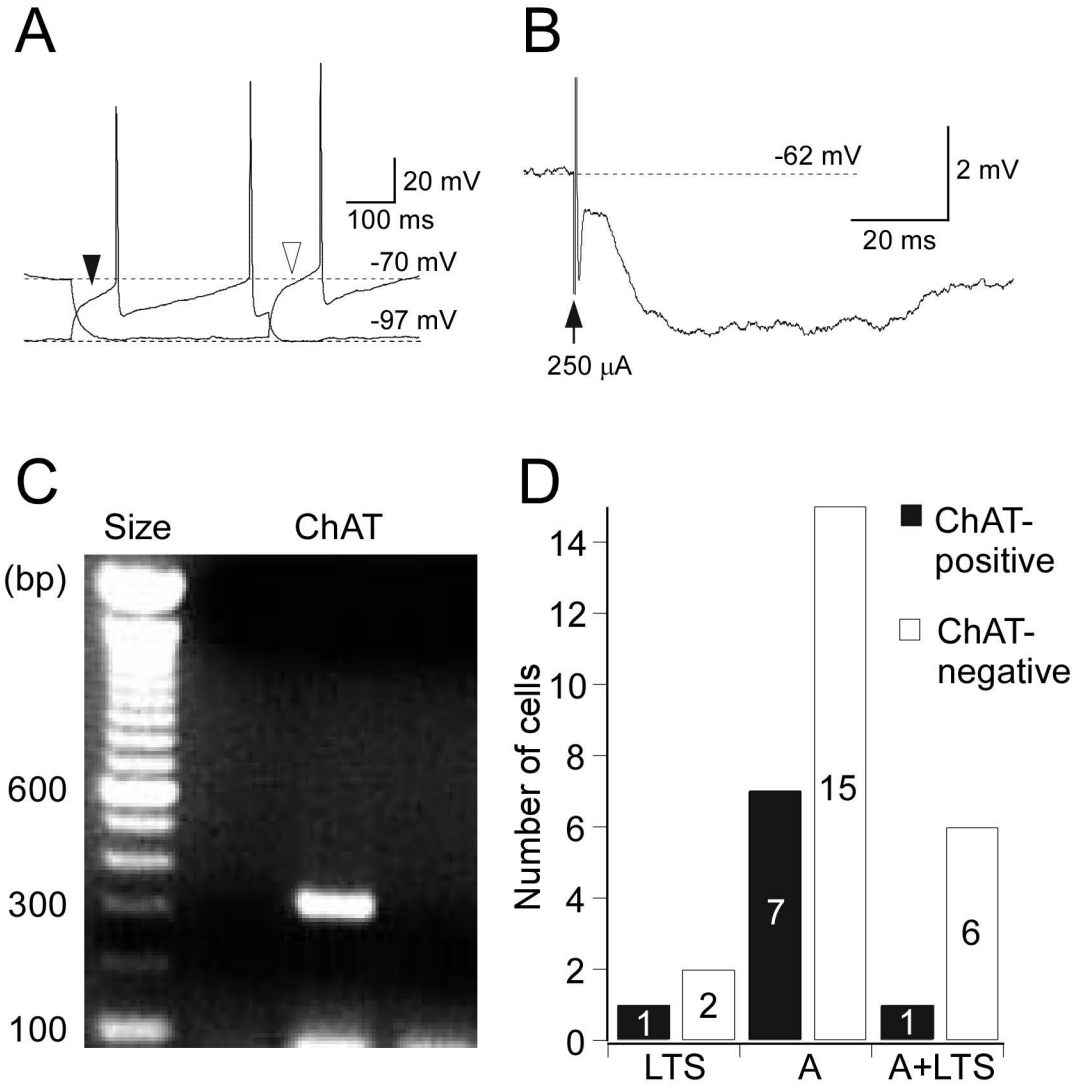
A
20 mV
100 ms
-70 mV
-97 mV
B
-62 mV
2 mV
20 ms
250 μA
C
Size
ChAT
(bp)
600
300
100
D
Number of cells
14
12
10
8
6
4
2
0
ChAT-positive
ChAT-negative
1
2
7
15
1
6
LTS
A
A+LTS